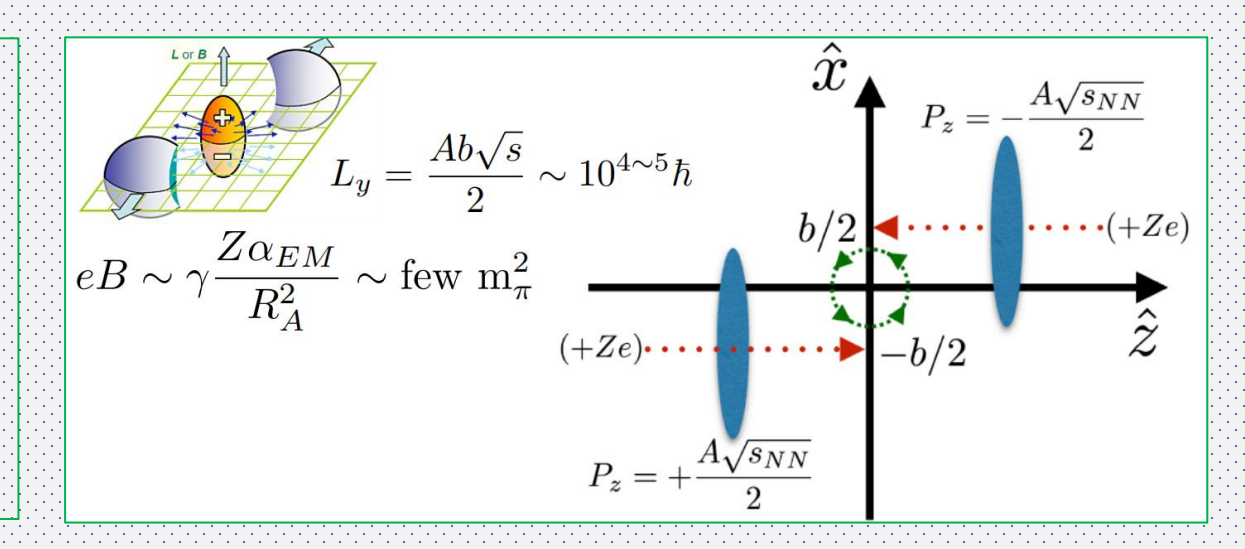
Spin Alignment and Phase Transition of QGP in the Presences of Magnetic and Vorticity Fields

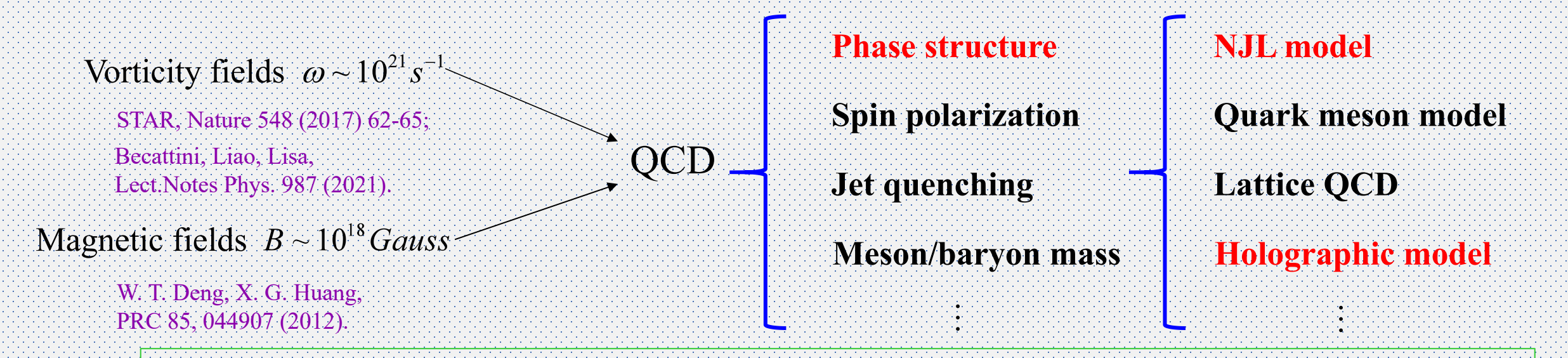
- 1. The Spin Alignment and Phase Structure of Thermal QGP under Rotation
- 2. The Anomalous Magnetic Moment and Phase Transition of the Magnetized QCD Background
- 3. Rotation Effect on the Deconfinement Phase Transition in Holographic QCD
- 4. Summary and Conclusions

Sheng-Qin Feng (冯笙琴) (Three Gorges Univ.)

Extremal Vorticity and Magnetic Fields in Relativistic HIC

For non-central high-energy collisions, the dense matter produced in the overlapped region of the collision will carry a global angular momentum along the direction opposite to the reaction plane (-y). Assuming that a partonic system is formed immediately following the initial collision, interactions among produced partons will lead to formation of a quark – gluon plasma (QGP).





1. The Spin Alignment and Phase Structure of Thermal QGP under Rotation

- (1) Y. Hua and S.-Q. Feng, Phys. Rev. D 111, 036012 (2025);
- (2) Y.-R. Bao and S.-Q. Feng, Phys. Rev. D 109, 096033 (2024).

From Gluon Topology to Quark Charality

$$Q_{w} = \frac{1}{32\pi^{2}} \int d^{4}x F^{a\mu\nu} \tilde{F}^{a}_{\mu\nu}$$

In the quark–gluon plasma (QGP), once these gluon configurations are excited at a certain spacetime point, the topological charge of the vacuum around that point will be altered by these gluon configurations. The chirality imbalance $N_5 = N_{\rm R} - N_{\rm L} = -2Q_{\rm w}$ is induced by the nonzero topological charge through the axial anomaly of QCD.

A non-zero $Q_{\rm W}$ will induce a corresponding fluctuation in the quark chiral imbalance N_5 . This process will result in chiral imbalance between right and left quarks, leading to the violation of parity (P) and charge-parity (CP) symmetry in the thermal plasma.

The effects of a chiral imbalance in a medium can be implemented in the grand canonical ensemble by introducing a chiral chemical potential μ_5 .

The Lagrangian of NJL model with the chiral chemical potential μ_5

The QCD matter produced in heavy-ion non-central collisions can rotate rapidly with local angular velocities ranging from 0.01 to 0.1 GeV. The Lagrangian of two flavors under the mean field approximation of the NJL model is given

chiral imbalance Orbital motion Spin motion
$$L_{MFA} = \overline{\psi} \left[i \gamma^{\mu} \partial_{\mu} - M + \mu \gamma^{0} + \mu_{5} \gamma^{0} \gamma^{5} + (\gamma^{0})^{-1} \left((\vec{\omega} \times \vec{x}) \cdot (-i\vec{\partial}) + \vec{\omega} \cdot \vec{S}_{4\times 4} \right) \right] - G_{s} \sigma^{2}$$

In cylindrical coordinates, the general positive-energy solutions for the quark field from the Dirac equation

corresponding to the above Lagrangian is given as

Reference:

- (1). Y. Jiang and J. Liao, Phys. Rev. Lett. 117, 192302 (2016);
- (2). Y. Hua and S.-Q. Feng, Phys. Rev. D 111, 036012 (2025)

$$\psi(\theta,r) = e^{-iEt + iP_z z} \begin{pmatrix} ce^{in\theta} J_n(p_t r) \\ ide^{i(n+1)\theta} J_{n+1}(p_t r) \\ c'e^{in\theta} J_n(p_t r) \\ id'e^{i(n+1)\theta} J_{n+1}(p_t r) \end{pmatrix}$$

The energy level, thermodynamic potential and chiral charge density

Through the calculation of the finite temperature field, the energy level and thermodynamic potential by rotation are obtained as follows:

$$E_{n,s} = \sqrt{\left(\sqrt{p_t^2 + p_z^2} - s\mu_5\right)^2 + M^2} - \left(n + \frac{1}{2}\right)\omega$$

$$\Omega = \frac{\left(M - m\right)^2}{4G_s} - \frac{N_f N_c}{8\pi^2} \sum_{n = -\infty}^{+\infty} \sum_{s = \pm 1}^{+\infty} \int dp_i^2 dp_z W_{n,s} \left\{ E_{n,s} + T \ln\left[1 + e^{-\beta(E_{n,s} - u)}\right] + T \ln\left[1 + e^{-\beta(E_{n,s} + u)}\right] \right\}$$

$$W_{n,s} = \left[J_n^2 \left(p_t r\right) + \lambda^2 J_{n+1}^2 \left(p_t r\right)\right] / \left(1 + \lambda^2\right)$$

Gap equation: $\frac{\partial \Omega}{\partial M} = 0$, $\frac{\partial^2 \Omega}{\partial M^2} > 0$

$$\frac{\partial \Omega}{\partial M} = 0, \quad \frac{\partial^2 \Omega}{\partial M^2} > 0$$

The chiral charge density n_5 is defined by :

$$\boldsymbol{n}_5 = -\frac{\partial \Omega}{\partial \mu_5}$$

Spin Alignment of ρ Mesons

The ρ meson is a vector meson composed of a quark and an antiquark with parallel spins (total spin s = 1). In extreme environments such as the rotating quarkgluon plasma (QGP) produced in noncentral heavy-ion collisions, ρ mesons may exhibit spin alignment — a phenomenon where their spin states correlate with the direction of system rotation.

The key observable for studying spin alignment is the spin density matrix element ρ_{00} , which describes the probability of the meson being in the spin states $s_7 = 0$. In the absence of polarization, $\rho_{00} = 1/3$ indicating isotropic spin distribution. A deviation from 1/3 signals spin polarization along a specific direction.

Spin Alignment of ρ Mesons

The spin alignment ρ_{00} is derived using a quark recombination model, where polarized quarks and antiquarks combine to form ρ mesons:

$$ho_{00} = rac{1 - P_q P_{ar{q}}}{3 + P_q P_{ar{q}}} pprox rac{1}{3} - rac{4}{9} P_q P_{ar{q}}$$

 P_q and $P_{\overline{q}}$ are the polarization of quarks and antiquarks, respectively.



Spin Alignment of ρ Mesons

According to the quark recombination model [1, 2], the spin alignment of fermions is composed of the particle number densities of quarks and antiquarks, which is given by the partial derivative of the thermodynamic potential with respect to the chemical potential:

$$N_{\uparrow}^{+} = \frac{N_{f}N_{e}}{4\pi^{2}} \sum_{n=-\infty}^{+\infty} \sum_{s=\pm 1}^{+\infty} \int dp_{t}dp_{z}p_{t} \frac{J_{n}^{2}(p_{t}r)}{1+\lambda^{2}} \frac{e^{-\beta(E_{n,s}-\mu)}}{1+e^{-\beta(E_{n,s}-\mu)}} \qquad N_{\downarrow}^{+} = \frac{N_{f}N_{e}}{4\pi^{2}} \sum_{n=-\infty}^{+\infty} \sum_{s=\pm}^{+\infty} \int dp_{t}dp_{z}p_{t} \frac{\lambda^{2}J_{n+1}^{2}(p_{t}r)}{1+\lambda^{2}} \frac{e^{-\beta(E_{n,s}-\mu)}}{1+e^{-\beta(E_{n,s}-\mu)}}$$

$$N_{\downarrow}^{+} = \frac{N_{f} N_{c}}{4\pi^{2}} \sum_{n=-\infty}^{+\infty} \sum_{s=\pm} \int dp_{t} dp_{z} p_{t} \frac{\lambda^{2} J_{n+1}^{2} (p_{t} r)}{1+\lambda^{2}} \frac{e^{-\beta(E_{n,s}-\mu)}}{1+e^{-\beta(E_{n,s}-\mu)}}$$

$$N_{\uparrow}^{-} = -\frac{N_{f} N_{c}}{4\pi^{2}} \sum_{n=-\infty}^{+\infty} \sum_{s=\pm 1} \int dp_{t} dp_{z} p_{t} \frac{J_{n}^{2}(p_{t}r)}{1+\lambda^{2}} \frac{e^{-\beta(E_{n,s}+\mu)}}{1+e^{-\beta(E_{n,s}+\mu)}}$$

$$N_{\uparrow}^{-} = -\frac{N_{f}N_{c}}{4\pi^{2}} \sum_{n=-\infty}^{+\infty} \sum_{s=\pm 1}^{+\infty} \int dp_{t} dp_{z} p_{t} \frac{J_{n}^{2}(p_{t}r)}{1+\lambda^{2}} \frac{e^{-\beta(E_{n,s}+\mu)}}{1+e^{-\beta(E_{n,s}+\mu)}} \qquad N_{\downarrow}^{-} = -\frac{N_{f}N_{c}}{4\pi^{2}} \sum_{n=-\infty}^{+\infty} \sum_{s=\pm 1}^{+\infty} \int dp_{t} dp_{z} p_{t} \frac{\lambda^{2}J_{n+1}^{2}(p_{t}r)}{1+\lambda^{2}} \frac{e^{-\beta(E_{n,s}+\mu)}}{1+e^{-\beta(E_{n,s}+\mu)}}$$

- [1] Z.-T. Liang and X.-N. Wang, Phys. Rev. Lett. 94, 102301 (2005);
- [2] Z.-T. Liang and X.-N. Wang, Phys. Lett. B 629, 20 (2005).



Comparison with other models

When studying the spin alignment of vector mesons ρ , besides our quark recombination model, there is also the quark condensation model [1]. The spin alignment corresponding to vector mesons ρ can take the

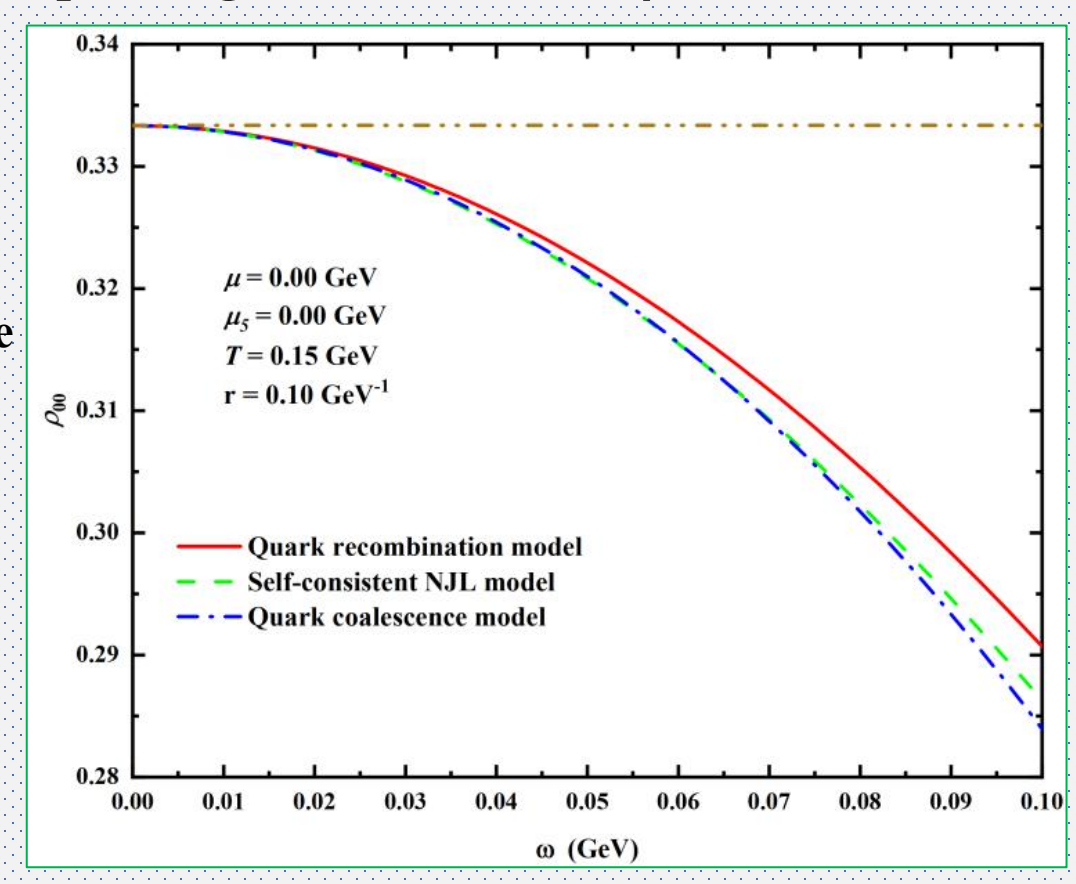
following form

$$\rho_{00} = \frac{1}{3} - \frac{4}{9} (\beta \omega)^2$$

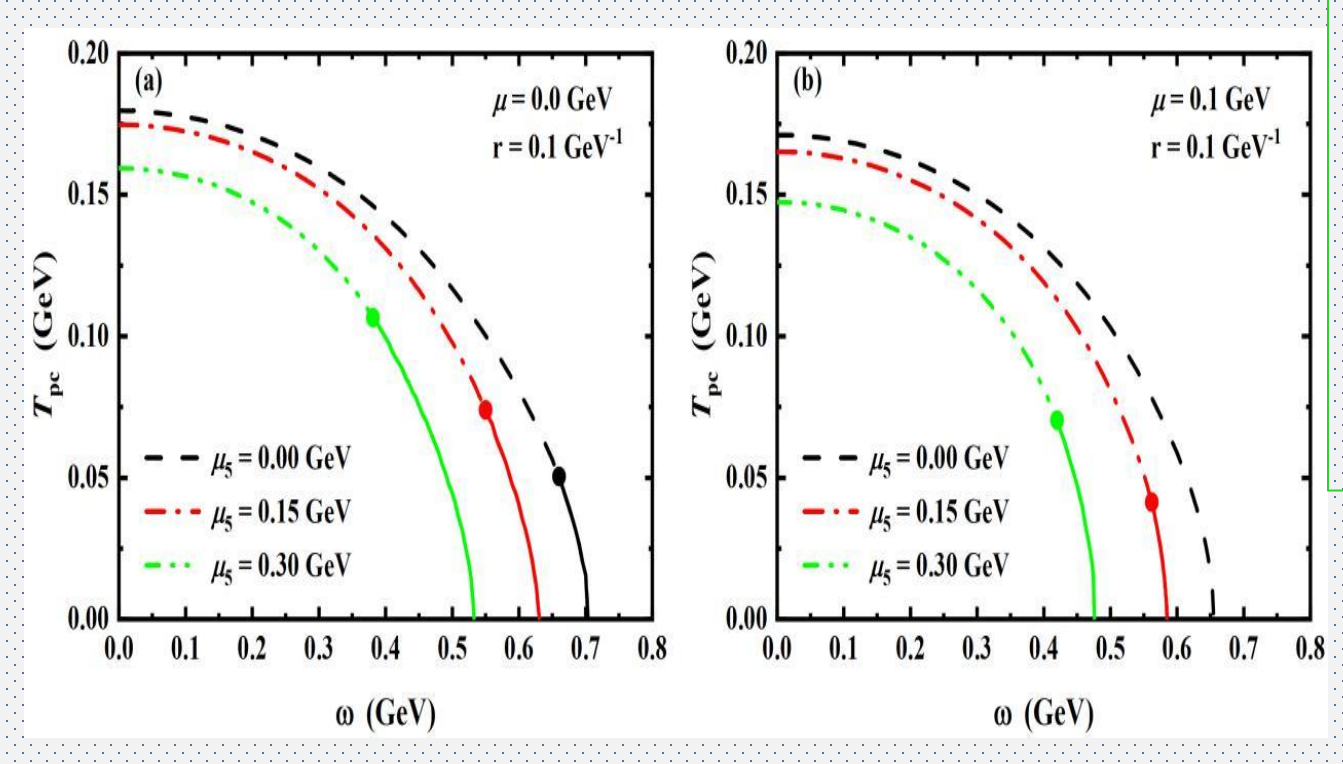
Another spin polarization model is self-consistent NJL model [2], the alignment of vector mesons (including ρ and ϕ) (T=150 MeV), exhibits the following relationship:

$$\rho_{00} = \frac{1}{3} - 5.10\omega^2 + 39.62\omega^4$$

[1] Y.-G. Yang, R.-H. Fang, Q. Wang, and X.-N. Wang, Phys. Rev. C 97, 034917(2018); [2] M. Wei and M. Huang, Chin. Phys. C 47, 104105(2023).



The phase structure of T - ω plane with chiral chemical potential

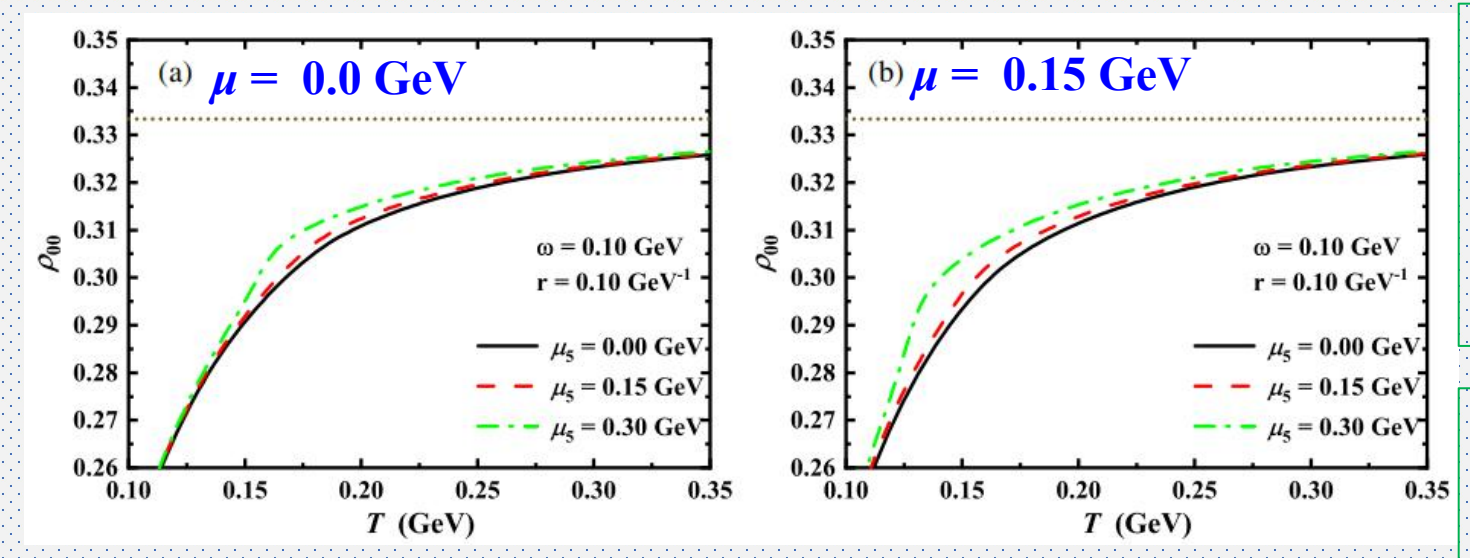


Y. Hua and S.-Q. Feng, Phys. Rev. D 111, 036012 (2025).

This figure illustrates the chiral phase diagram in the $T_{\rm pc}-\omega$ plane for varying chiral chemical potentials μ_5 . The critical temperature $T_{\rm pc}$ decreases with increasing μ_5 , but the critical end point (CEP) shifts toward higher T and lower ω .

It resolves how chiral imbalance alters the order and criticality of the chiral phase transition under rotation, providing insights into the interplay of vorticity and parity violation in quark-gluon plasma (QGP).

The relationship between spin alignment ρ_{00} and temperature T



Spin alignment ρ_{00} of ρ mesons as a function of temperature T

 ρ_{00} approaches 1/3 (isotropic spin alignment) at high T, while deviating 1/3 near the phase transition temperature.

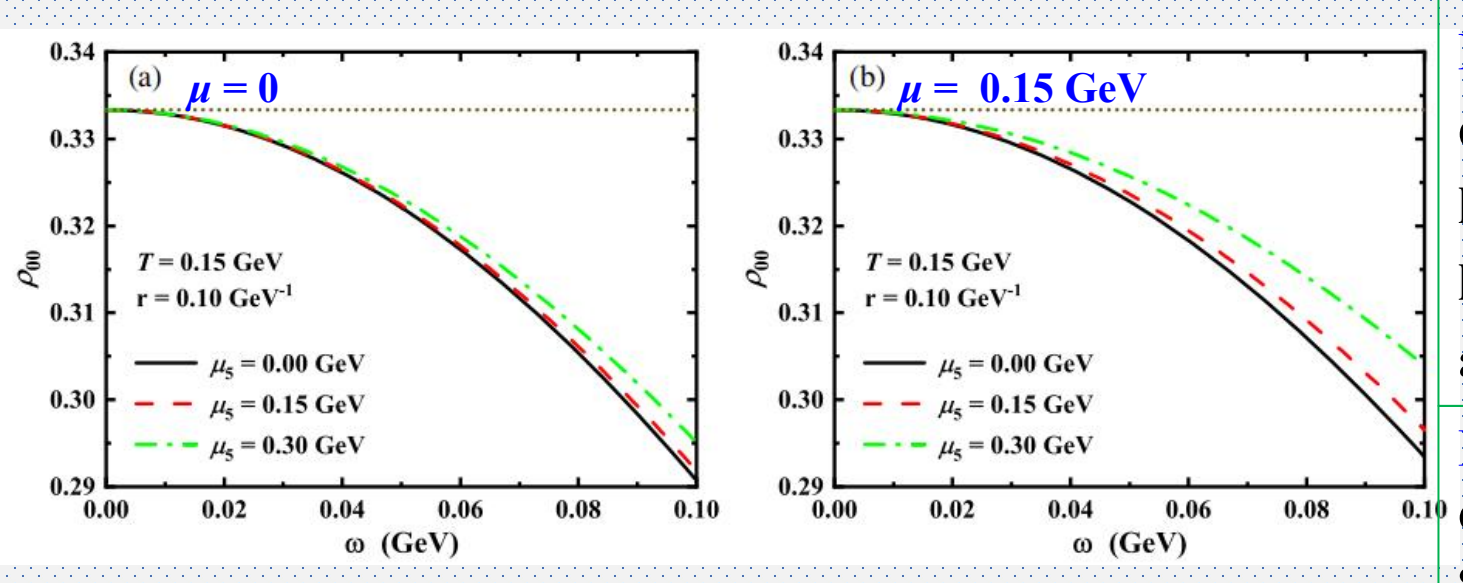
Increasing μ_5 enhances ρ_{00} , reducing spin polarization.

Innovation & Impact: This is the first work to connect chiral imbalance (μ_5) with vector meson spin alignment, showing that μ_5 counteracts rotation-induced polarization near $T_{\rm pc}$.

Y. Hua and S.-Q. Feng, Phys. Rev. D 111, 036012 (2025).

Key Problem Solved: It explains how chiral imbalance moderates spin polarization in a temperature-dependent manner, crucial for interpreting experimental ρ_{00} data in QGP.

The relationship between spin alignment ρ_{00} and rotational velocity ω



Spin alignment ρ_{00} of ρ mesons as a function of ω

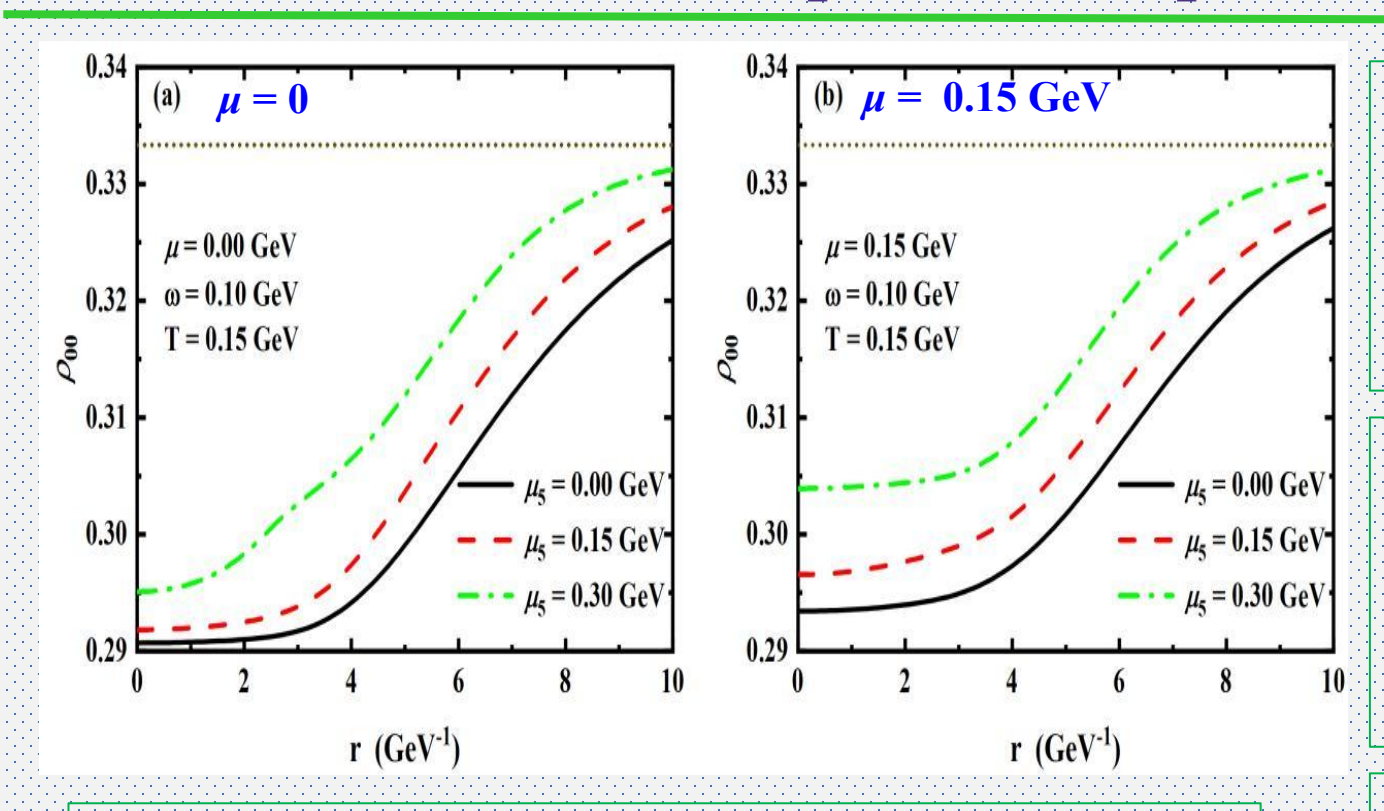
Research Content: ρ_{00} decreases with ω , deviating from 1/3 (indicating polarization). large ω makes more polarization, but larger μ_5 reduces this deviation, particularly at high ω , makes less polarization.

Innovation & Impact: It demonstrates that chiral imbalance suppresses rotation-induced spin polarization, offering a mechanism to tune meson spin states via μ_5

Key Problem Solved: It resolves how competing effects of rotation and chiral imbalance determine the net polarization of vector mesons, vital for probing spin-orbit coupling in QCD matter.

Y. Hua and S.-Q. Feng, Phys. Rev. **D** 111, 036012 (2025).

The relationship between spin alignment ρ_{00} and rational radius



Research Content: ρ_{00} increases with r, approaching 1/3, showing reduced polarization away from the rotation center. μ_5 enhances ρ_{00} at all r, especially near $T_{\rm pc}$.

Innovation & Impact: This study pioneers the spatial analysis of spin alignment in rotating systems, revealing radial gradients in polarization and the moderating role of μ_5 .

Spin alignment ρ_{00} of ρ mesons as a function of radius r

Y. Hua and S.-Q. Feng, Phys. Rev. D 111, 036012 (2025).

Key Problem Solved: It identifies the spatial inhomogeneity of spin polarization in vortical QGP, essential for understanding local spin dynamics in finite-size systems like heavy-ion collisions.

2. Anomalous Magnetic Moment (AMM) and Phase transition in Magnetized QCD Matter

- (1) C.-Y. Yang and S.-Q. Feng, Phys. Rev. D 112, 036008 (2025);
- (2) X.-Q. Zhu and S.-Q. Feng, Phys. Rev. D 107, 016018 (2023);
- (3) Y.-W. Qiu and S.-Q. Feng, X.-Q. Zhu, Phys. Rev. D 108, 116022 (2023)

The SU(3) NJL model with quark anomalous magnetic moment (AMM)

Lagrangian density (three flavors, broken isospin symmetry)

Landau gauge $A_{\mu} = (0,0,xB,0)$

$$\mathcal{L}_{NJL} = \sum_{f=u,d,s} \bar{\psi}_f (i\gamma^{\mu} D_{\mu}^{(f)} - m_f - \frac{1}{2} e_f \kappa_f \sigma^{\mu\nu} F_{\mu\nu}) \psi_f + \frac{\mathbf{M. Str}}{12503}$$

$$G \sum_{a=0}^{8} [(\bar{\psi} \lambda_a \psi)^2 + (\bar{\psi} i \gamma^5 \lambda_a \psi)^2] - K(\det[\bar{\psi}(1+\gamma^5)\psi] + \det[\bar{\psi}(1-\gamma^5)\psi])$$

M. Strickland, V. Dexheimer, and D. P. Menezes, Phys. Rev.D 86, 125032 (2012).

The contribution of the anomalous magnetic moment (AMM) to the Lagrangian density does

arise from the interaction between the AMM and the quark spin.

In the NJL Lagrangian used, the AMM term is: $-\frac{1}{2}e_f\kappa_f\sigma^{\mu\nu}F_{\mu\nu}$

$$-rac{1}{2}e_f\kappa_f\sigma^{\mu
u}F_{\mu
u}$$

- $\sigma^{\mu\nu}=\frac{i}{2}[\gamma^{\mu},\gamma^{\nu}]$ is the **spin tensor operator**, which is directly related to the quark's spin structure.
- $F_{\mu\nu}$ is the electromagnetic field strength tensor.
- κ_f is the flavor-dependent AMM of the quark.

The SU(3) NJL model with quark anomalous magnetic moment (AMM)

Mean-field approximation:

Thermodynamic potential:
$$\Omega_{MF} = \Omega_q + 2G(\sigma_u^2 + \sigma_d^2 + \sigma_s^2) - 4K\sigma_u\sigma_d\sigma_s$$

where:
$$\Omega_q = -3 \sum_{f=u,d,s} \frac{|q_f B|}{2\pi} \sum_n \sum_{s=\pm 1} \int \frac{dp_z}{2\pi} [E_{fns} + T \ln \left(1 + e^{-\frac{E_{fns} + \mu}{T}}\right) + T \ln \left(1 + e^{-\frac{E_{fns} - \mu}{T}}\right)]$$

Gap eqs:
$$\partial \Omega_{MF}/\partial \sigma_f = 0$$
 $\Longrightarrow M_f = m_f - 4G\sigma_f + 2K\prod_{f'=f} \sigma_{f'}$ minimizing: Ω_{MF}

Chiral condensates: $\sigma_f = \langle \bar{\psi}_f \psi_f \rangle = -\frac{|e_f B|}{(2\pi)^2} \int dp_z \sum_{E_{fns}} \frac{M_f}{E_{fns}} (1 - \frac{s\kappa_f e_f B}{M_{nf}}) (1 - \frac{1}{e^{(E_{fns} - \mu)/T} + 1} - \frac{1}{e^{(E_{fns} + \mu)/T} + 1})$

Energy eigenvalue:
$$E_{fns} = \sqrt{p_z + (M_{nf} - s\kappa_f e_f B)^2}, M_{nf} = \sqrt{M_f^2 + 2n|e_f B|}$$

The SU(3) NJL model with quark AMM

Transforming the six-fermion interaction into an effective four-fermion interaction,

> one obtains:

$$\mathcal{L}_{NJL} = \sum_{f=u,d,s} \bar{\psi}_{f} (i\gamma^{\mu} D_{\mu}^{(f)} - m_{f} - \frac{1}{2} e_{f} \kappa_{f} \sigma^{\mu\nu} F_{\mu\nu}) \psi_{f}$$

$$+ \sum_{a=0}^{8} [K_{a}^{-} (\bar{\psi} \lambda_{a} \psi)^{2} + K_{a}^{+} (\bar{\psi} i \gamma^{5} \lambda_{a} \psi)^{2}]$$

$$+ K_{30}^{-} (\bar{\psi} \lambda_{3} \psi) (\bar{\psi} \lambda_{0} \psi) + K_{30}^{+} (\bar{\psi} i \gamma^{5} \lambda_{3} \psi) (\bar{\psi} i \gamma^{5} \lambda_{0} \psi)$$

$$+ K_{80}^{-} (\bar{\psi} \lambda_{8} \psi) (\bar{\psi} \lambda_{0} \psi) + K_{80}^{+} (\bar{\psi} i \gamma^{5} \lambda_{8} \psi) (\bar{\psi} i \gamma^{5} \lambda_{0} \psi)$$

$$+ K_{83}^{-} (\bar{\psi} \lambda_{8} \psi) (\bar{\psi} \lambda_{3} \psi) + K_{83}^{+} (\bar{\psi} i \gamma^{5} \lambda_{8} \psi) (\bar{\psi} i \gamma^{5} \lambda_{3} \psi)$$

$$+ K_{03}^{-} (\bar{\psi} \lambda_{0} \psi) (\bar{\psi} \lambda_{3} \psi) + K_{03}^{+} (\bar{\psi} i \gamma^{5} \lambda_{0} \psi) (\bar{\psi} i \gamma^{5} \lambda_{3} \psi)$$

$$+ K_{08}^{-} (\bar{\psi} \lambda_{0} \psi) (\bar{\psi} \lambda_{8} \psi) + K_{08}^{+} (\bar{\psi} i \gamma^{5} \lambda_{0} \psi) (\bar{\psi} i \gamma^{5} \lambda_{8} \psi)$$

$$+ K_{38}^{-} (\bar{\psi} \lambda_{3} \psi) (\bar{\psi} \lambda_{8} \psi) + K_{38}^{+} (\bar{\psi} i \gamma^{5} \lambda_{3} \psi) (\bar{\psi} i \gamma^{5} \lambda_{8} \psi)$$

$$+ K_{38}^{-} (\bar{\psi} \lambda_{3} \psi) (\bar{\psi} \lambda_{8} \psi) + K_{38}^{+} (\bar{\psi} i \gamma^{5} \lambda_{3} \psi) (\bar{\psi} i \gamma^{5} \lambda_{8} \psi)$$

Effective coupling constants:

$$K_0^{\pm} = G \pm \frac{1}{3} K(\sigma_u + \sigma_d + \sigma_s),$$

$$K_1^{\pm} = K_2^{\pm} = K_3^{\pm} = G \pm \frac{1}{2} K \sigma_s,$$

$$K_4^{\pm} = K_5^{\pm} = G \pm \frac{1}{2} K \sigma_d,$$

$$K_6^{\pm} = K_7^{\pm} = G \pm \frac{1}{2} K \sigma_u,$$

$$K_8^{\pm} = G \pm \frac{1}{6} K(2\sigma_u + 2\sigma_d - \sigma_s),$$

$$K_{30}^{\pm} = K_{03}^{\pm} = \mp \frac{1}{2\sqrt{6}} K(\sigma_u - \sigma_d),$$

$$K_{80}^{\pm} = K_{08}^{\pm} = \pm \frac{\sqrt{2}}{12} K(\sigma_u + \sigma_d - 2\sigma_s),$$

$$K_{83}^{\pm} = K_{38}^{\pm} = \pm \frac{1}{2\sqrt{3}} K(\sigma_u - \sigma_d),$$

Chiral condensates: $\sigma_u = \langle \bar{\psi}_u \psi_u \rangle, \sigma_d = \langle \bar{\psi}_d \psi_d \rangle, \sigma_s = \langle \bar{\psi}_s \psi_s \rangle$

Ideas:

(1) Quarks: mean-field



(2) Mesons: RPA resummation (quantum fluctuation)

$$\Rightarrow = = = = < \simeq \times + \times \times + \times \times + \times \times \times = \frac{\times}{1 - \times}$$

S. Klevansky, Rev. Mod. Phys. 64, 649 (1992). M. Buballa, Phys. Rept. 407, 205 (2005)

Presenting the calculation results directly:

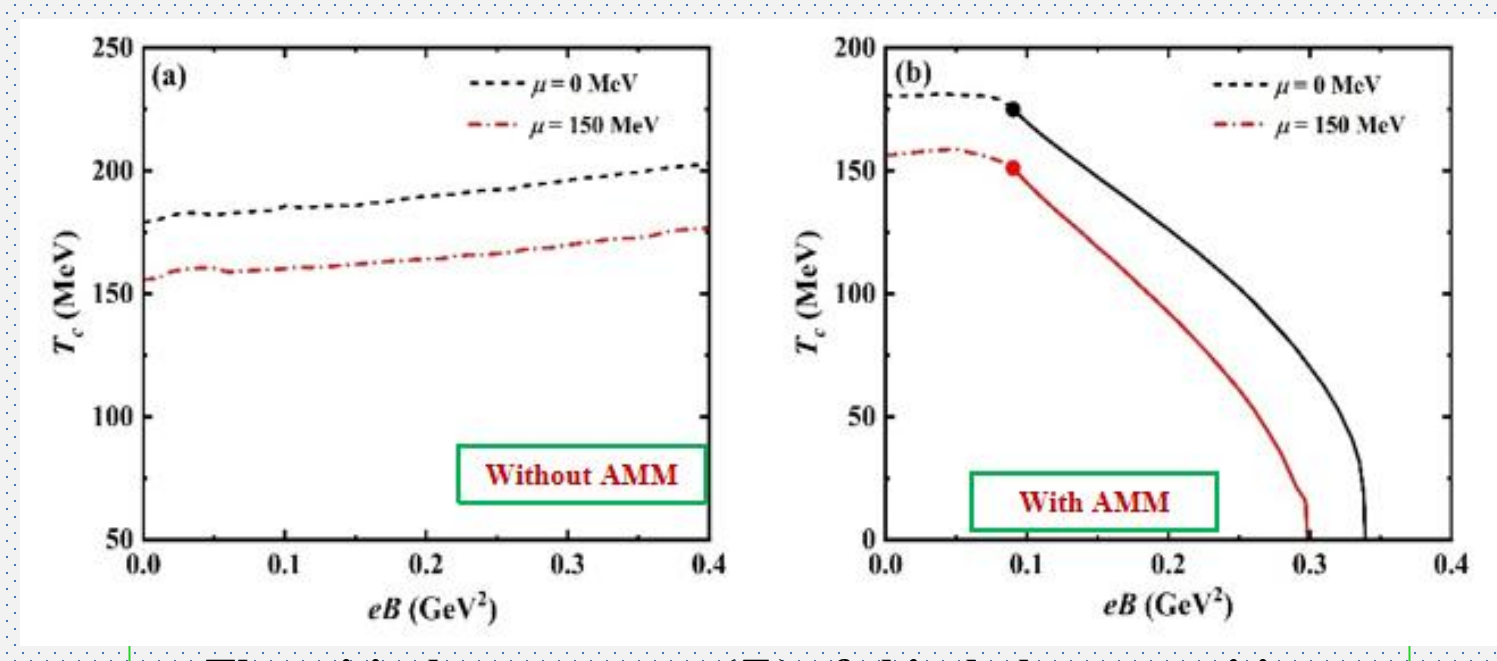
K meson:
$$M = \frac{2K_6^+}{1 - 2K_6^+ \Pi_{K^0}^{ps}(p)}$$

$$\text{Where} \qquad \int dk_z \left\{ \frac{1}{E_{dns}} \left[\frac{1}{(E_{dns} + p_0)^2 - E_{snl}^2} \frac{1}{e^{-(E_{dns} + \mu)/T}} \right] \right. \\ \left. \int dk_z \left\{ \frac{1}{E_{dns}} \left[\frac{1}{(E_{dns} + p_0)^2 - E_{snl}^2} \frac{1}{e^{-(E_{dns} + \mu)/T}} \right] \right. \\ \left. \int dk_z \left\{ \int dk_z \frac{1}{E_{dns}} \left[1 - \frac{1}{e^{(E_{dns} - \mu)/T} + 1} - \frac{1}{e^{(E_{dns} + \mu)/T} + 1} \right] \right. \\ \left. + \int dk_z \frac{1}{E_{snl}} \left[1 - \frac{1}{e^{(E_{snl} - \mu)/T} + 1} - \frac{1}{e^{(E_{snl} + \mu)/T} + 1} \right] \right. \\ \left. + \int dk_z \frac{1}{E_{snl}} \left[1 - \frac{1}{e^{(E_{snl} - \mu)/T} + 1} - \frac{1}{e^{(E_{snl} + \mu)/T} + 1} \right] \right. \\ \left. + \int dk_z \frac{1}{E_{snl}} \left[1 - \frac{1}{e^{(E_{snl} - \mu)/T} + 1} - \frac{1}{e^{(E_{snl} + \mu)/T} + 1} \right] \right. \\ \left. + \int dk_z \frac{1}{E_{snl}} \left[1 - \frac{1}{e^{(E_{snl} - \mu)/T} + 1} - \frac{1}{e^{(E_{snl} + \mu)/T} + 1} \right] \right. \\ \left. + \int dk_z \frac{1}{E_{snl}} \left[1 - \frac{1}{e^{(E_{snl} - \mu)/T} + 1} - \frac{1}{e^{(E_{snl} - \mu)/T} + 1} \right] \right\} \right. \\ \left. + \int dk_z \frac{1}{E_{snl}} \left[1 - \frac{1}{e^{(E_{snl} - \mu)/T} + 1} - \frac{1}{e^{(E_{snl} - \mu)/T} + 1} \right] \right. \\ \left. + \int dk_z \frac{1}{E_{snl}} \left[1 - \frac{1}{e^{(E_{snl} - \mu)/T} + 1} - \frac{1}{e^{(E_{snl} - \mu)/T} + 1} \right] \right. \\ \left. + \int dk_z \frac{1}{E_{snl}} \left[1 - \frac{1}{e^{(E_{snl} - \mu)/T} + 1} - \frac{1}{e^{(E_{snl} - \mu)/T} + 1} \right] \right. \\ \left. + \int dk_z \frac{1}{E_{snl}} \left[1 - \frac{1}{e^{(E_{snl} - \mu)/T} + 1} - \frac{1}{e^{(E_{snl} - \mu)/T} + 1} \right] \right. \\ \left. + \int dk_z \frac{1}{E_{snl}} \left[1 - \frac{1}{e^{(E_{snl} - \mu)/T} + 1} - \frac{1}{e^{(E_{snl} - \mu)/T} + 1} \right] \right. \\ \left. + \int dk_z \frac{1}{E_{snl}} \left[1 - \frac{1}{e^{(E_{snl} - \mu)/T} + 1} - \frac{1}{e^{(E_{snl} - \mu)/T} + 1} \right] \right] \right. \\ \left. + \int dk_z \frac{1}{E_{snl}} \left[1 - \frac{1}{e^{(E_{snl} - \mu)/T} + 1} - \frac{1}{e^{(E_{snl} - \mu)/T} + 1} \right] \right] \right. \\ \left. + \int dk_z \frac{1}{E_{snl}} \left[1 - \frac{1}{e^{(E_{snl} - \mu)/T} + 1} - \frac{1}{e^{(E_{snl} - \mu)/T} + 1} \right] \right] \right. \\ \left. + \int dk_z \frac{1}{E_{snl}} \left[1 - \frac{1}{e^{(E_{snl} - \mu)/T} + 1} - \frac{1}{e^{(E_{snl} - \mu)/T} + 1} \right] \right] \right. \\ \left. + \int dk_z \frac{1}{E_{snl}} \left[1 - \frac{1}{e^{(E_{snl} - \mu)/T} + 1} - \frac{1}{e^{(E_{snl} - \mu)/T} + 1} \right] \right. \\ \left. + \int dk_z \frac{1}{E_{snl}} \left[1 - \frac{1}{e^{(E_{snl} - \mu)/T} + 1} - \frac{1}{e^{(E_{snl} - \mu)/T} + 1} \right] \right] \right. \\ \left. + \int dk_z \frac{1}{E_{snl}} \left[1 - \frac{1}{e^{(E_{snl} - \mu)/T$$

+ $\{[(M_{nd} - s\kappa_d e_d B) - sl(M_{ns} - l\kappa_s e_s B)]^2 - p_0^2\} B(m_d, m_s)\}$

$$B(m_d, m_s) = \int dk_z \left\{ \frac{1}{E_{dns}} \left[\frac{1}{(E_{dns} + p_0)^2 - E_{snl}^2} \frac{1}{e^{-(E_{dns} + \mu)/T} + 1} \right] - \frac{1}{(E_{dns} - p_0)^2 - E_{snl}^2} \frac{1}{e^{(E_{dns} - \mu)/T} + 1} \right] + \frac{1}{E_{snl}} \left[\frac{1}{(E_{snl} - p_0)^2 - E_{dns}^2} \frac{1}{e^{-(E_{snl} + \mu)/T} + 1} \right] - \frac{1}{(E_{snl} + p_0)^2 - E_{dns}^2} \frac{1}{e^{(E_{snl} - \mu)/T} + 1} \right].$$

QCD Phase Diagram Restructuring



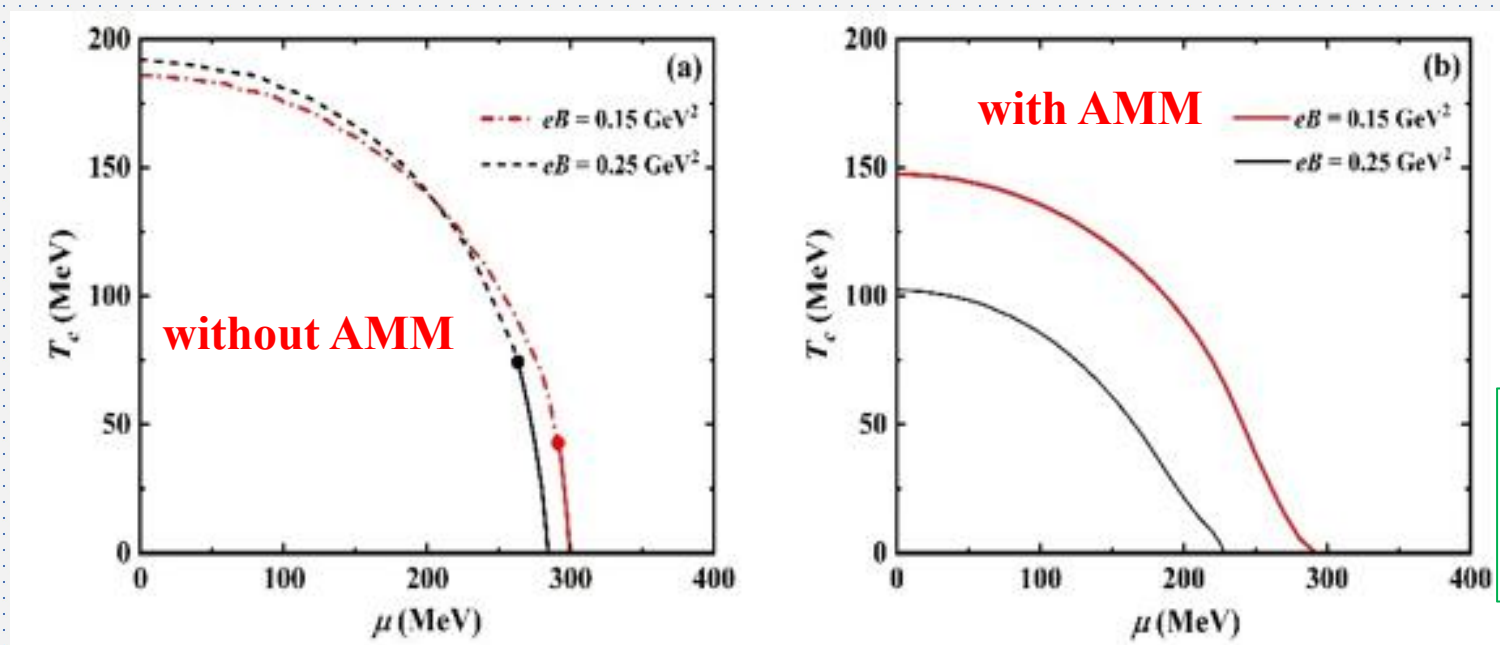
The critical temperature (T_c) of chiral phase transitions as a function of eB at different chemical potentials (μ) , with and without AMM.

- Magnetic catalysis without AMM
- Inverse magnetic catalysis with AMM
- Non-contradiction with LQCD calculation results.

(1) Phase Diagram Reshaping and **CEP Shift:** AMM suppresses T_c and shifts critical endpoints (CEP) toward lower eB and higher T, contrasting conventional NJL predictions dominated by magnetic catalysis (MC). (2) Crossover-to-First-Order Transition: AMM replaces crossover transitions with first-order transitions under strong eB, validating AMM's role in altering phase transition sequences in multi-flavor systems.

- (1) C.-Y. Yang and S.-Q. Feng, Phys. Rev. D 112, 036008 (2025);
- (2) X.-Q. Zhu and S.-Q. Feng, Phys. Rev. D 107, 016018 (2023);
- (3) Y.-W. Qiu and S.-Q. Feng, X.-Q. Zhu, Phys. Rev. D 108, 116022 (2023).

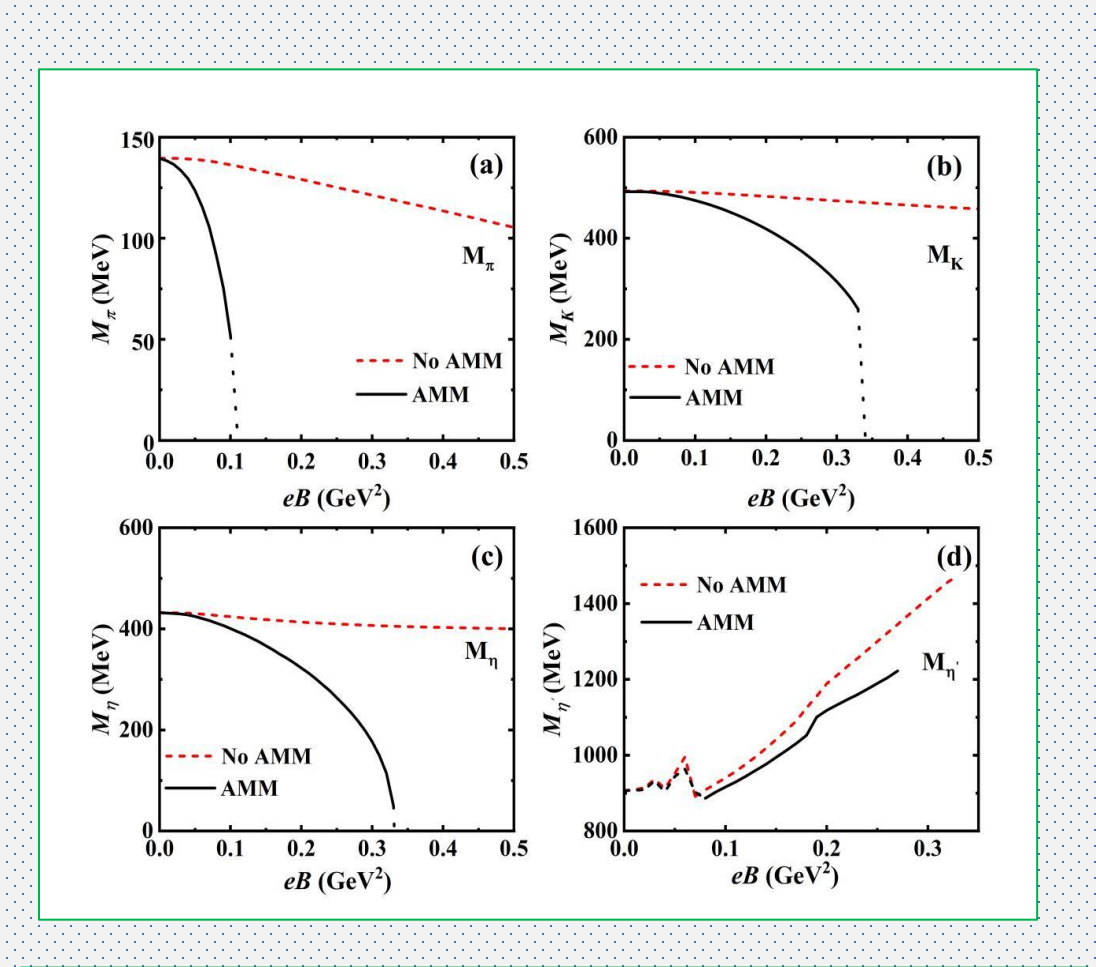
QCD Phase Diagram Restructuring



The critical temperature (T_c) for chiral phase transition as a function of chemical potential for different magnetic fields

- (1) C.-Y. Yang and S.-Q. Feng, Phys. Rev. D 112, 036008 (2025);
- (2) X.-Q. Zhu and S.-Q. Feng, Phys. Rev. D 107, 016018 (2023);
- (3) Y.-W. Qiu and S.-Q. Feng, X.-Q. Zhu, Phys. Rev. D 108, 116022 (2023);
- Crossover transitions into first-order transitions without AMM
- Uniform manifestation as first-order phase transitions with AMM
- T_c is a decreasing function of μ

The magnetic dependences of neutral pseudoscalar meson mass spectra



- (1) C.-Y. Yang and S.-Q. Feng, Phys. Rev. D 112, 036008 (2025);
- (2) X.-Q. Zhu and S.-Q. Feng, Phys. Rev. D 107, 016018 (2023).

- (1) Meson Mass Collapse and Chiral Restoration: AMM triggers abrupt mass collapses (e.g., π at $eB \approx 0.1$ GeV²), directly linking meson stability to chiral symmetry restoration.
- (2) η' Resonance Limitations: η' mass diverges under strong eB due to non-perturbative decay width effects, exposing NJL's limitations in handling resonance states.

Key Issues Addressed:

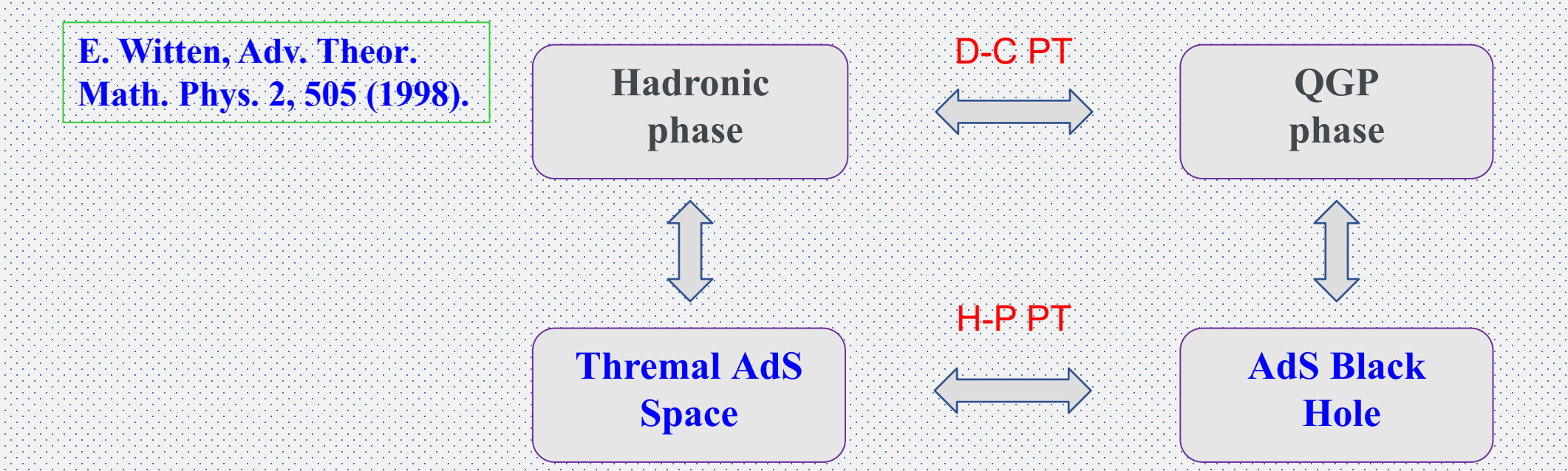
Systematically reveals AMM's role in regulating multi-flavor meson masses and flavor mixing (e.g., π^0 - η - η'), addressing gaps in two-flavor models' predictions for magnetic sensitivity.

3. Rotation effect on the deconfinement phase transition in holographic QCD

- (1) J.-H. Wang and S.-Q. Feng, Phys. Rev. D 109, 066019 (2024)
 - (2) J. Deng and S.-Q. Feng, Phys. Rev. D 105, 026015 (2022)

Hawking-Page Phase Transition

Confinement-Deconfinement Phase Transition in AdS/QCD



Research method

Holographic QCD: The holographic principle is used to study the phase transition of QCD, especially through the Einstein-Maxwell system.

The rotating metric: By introducing a metric with a rotating cylindrical coordinate system, we calculate the Hawking temperature and study the effect of rotation on phase transitions.

J.-H. Wang and S.-Q. Feng, Phys. Rev. D 109, 066019 (2024);

J. Deng and S.-Q. Feng, Phys. Rev. D 105, 026015 (2022).

Introducing of rotation effect

J.-H. Wang and S.-Q. Feng, Phys. Rev. D 109, 066019 (2024).

The rotating extension from the static configuration can be obtained through a local Lorentz boost as:

$$t \to \frac{1}{\sqrt{1 - l^2 \omega^2}} (t + l^2 \omega \phi) \qquad \phi \to \frac{1}{\sqrt{1 - l^2 \omega^2}} (\phi + \omega t)$$

The corresponding transformation of the metric is:

$$ds^{2} = g_{tt}dt^{2} + g_{t\phi}dtd\phi + g_{\phi t}d\phi dt + g_{\phi\phi}l^{2}d\phi^{2} + g_{zz}dz^{2} + g_{xx}\sum_{i=1}^{2}dx_{i}^{2}$$

To obtain the Hawking temperature of rotating black hole, we reestablish the above metric as:

$$ds^{2} = \frac{L^{2}}{z^{2}} \left[-N(z)^{2} f(z) dt^{2} + \frac{dz^{2}}{f(z)} + R(z) (d \phi + P(z) dt)^{2} + \sum_{i=1}^{2} dx_{i}^{2} \right] \qquad T_{H} = -\frac{N(z_{h}) f'(z_{h})}{4\pi}$$

$$\mu = \mu' \sqrt{1 - \omega^{2}}$$

The difference of the free energy density

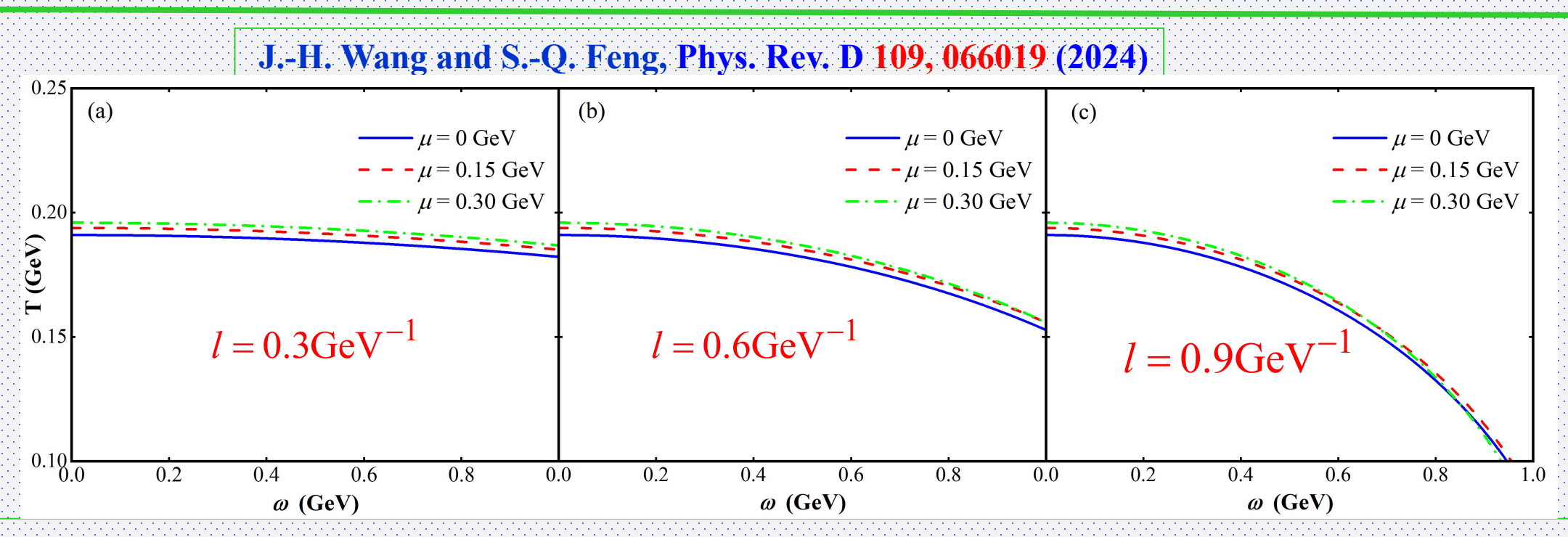
The action for soft wall model

$$S = \int d^{5}x \sqrt{G}e^{-\Phi} \left[\frac{1}{2\kappa^{2}} (-R + 2\Lambda) + \frac{1}{4g^{2}} F_{MN} F^{MN} \right]$$

The difference of the free energy density between the two geometrical backgrounds is:

$$\begin{split} \Delta F &= T\Delta \mathcal{E} \\ &= \frac{1}{24c\pi^2 z_h^{\ 4} (-1+\omega^2)} e^{-cz_h^2} N_c \\ &\quad (4(-1+e^{cz_h^2}) N_f \mu^2 - 2ce^{cz_h^2} N_f \mu^2 z_h^2 \\ &\quad + 3c(-2+e^{cz_h^2}) N_c (-1+\omega^2) - 6c^2 z_h^2 (N_c + \frac{3}{2} e^{cz_h^2} N_f z_h^2 \mu^2 - N_c \omega^2) \\ &\quad + 6c^3 e^{cz_h^2} N_c z_h^4 (-1+\omega^2) Ei(-cz_h^2)) \end{split}$$

The Phase transitions of rotations



- For small rotation radii, the phase transition temperature slightly decreases with the rotational angular velocity, but as the rotation radius increases, the phase transition temperature rapidly decreases with the rotational angular velocity.
- This study provides a new perspective for understanding the phase transition characteristics with the size of the rotating systems in strongly interacting matter, and may have guiding significance for future experimental observations.

4. Summary and Conclusions

Summary and conclusions

- 1. The spin alignment of η_{00} and phase structure of thermal QGP under rotation are investigated. It is found that chiral imbalance have some effects on phase structure of QGP medium. We also study some dependences of spin alignment of η_{00} with temperature, angular velocity, rotational radius on chiral imbalance.
- 2. The research investigates the impact of the anomalous magnetic moment (AMM) of quarks on the mass spectra of neutral pseudoscalar mesons (π, K, η, η') under conditions of strong magnetic fields, finite temperatures, and chemical potentials, based on the three-flavor Nambu-Jona-Lasinio (NJL) model.
- 3. The first holographic study on the influence of the radius of a homogeneous rotating system on the phase diagram is established in the article. As we are discussing the rotating system of QCD medium, the phase transition characteristics should depend on the finite size of the rotating system. Due to the cylindrical symmetry of the rotating system, the rotation radius *l* has become an important characteristic quantity of the rotating system.

Thanks!